

High-Quality 3D Head Reconstruction from Any Single Portrait Image

Jianfu Zhang¹, Yujie Gao¹, Jiahui Zhan¹, Wentao Wang², Haohua Zhao¹, Liqing Zhang¹

¹Shanghai Jiaotong University

²Shanghai AI Laboratory

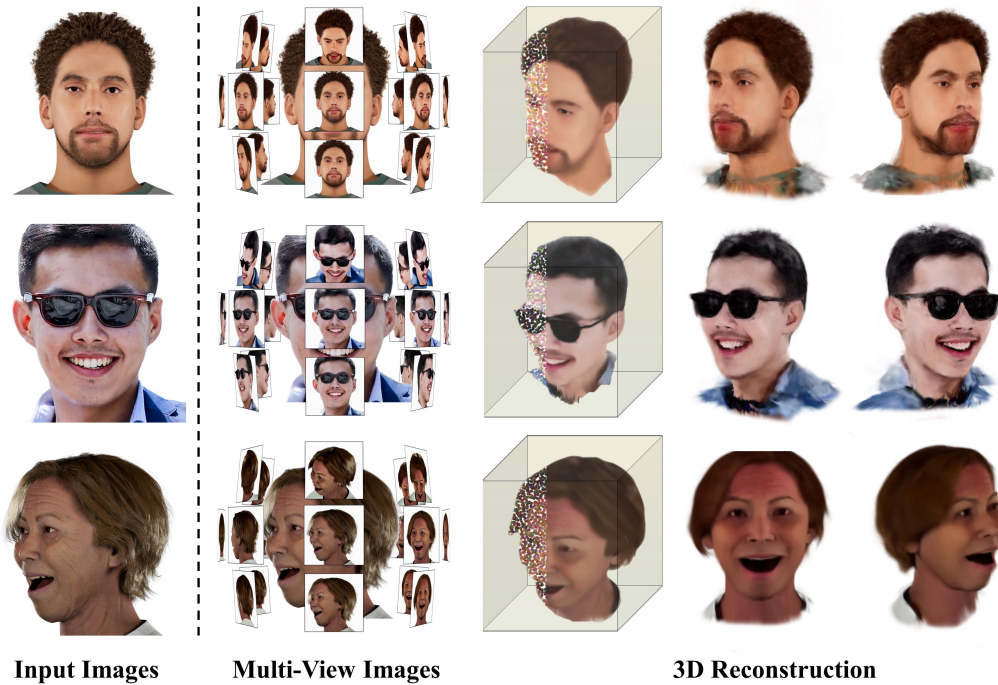


Figure 1: We generate a multi-view video around the head from a single portrait image. The 3D representation of the identity is then reconstructed using the multi-view video. Experiments show that our method performs well on identity and expression consistency even for side-face angles and when accessories are present.

Abstract

In this work, we introduce a novel high-fidelity 3D head reconstruction method from a single portrait image, regardless of perspective, expression, or accessories. Despite significant efforts in adapting 2D generative models for novel view synthesis and 3D optimization, most methods struggle to produce high-quality 3D portraits. The lack of crucial information, such as identity, expression, hair, and accessories, limits these approaches in generating realistic 3D head models. To address these challenges, we construct a new high-quality dataset containing 227 sequences of digital human portraits captured from 96 different perspectives, totalling

21,792 frames, featuring diverse expressions and accessories. To further improve performance, we integrate identity and expression information into the multi-view diffusion process to enhance facial consistency across views. Specifically, we apply identity- and expression-aware guidance and supervision to extract accurate facial representations, which guide the model and enforce objective functions to ensure high identity and expression consistency during generation. Finally, we generate an orbital video around the portrait consisting of 96 multi-view frames, which can be used for 3D portrait model reconstruction. Our method demonstrates robust performance across challenging scenarios, including side-face angles and complex ac-

cessories.

1 Introduction

Synthesizing 3D portraits with arbitrary expressions has widespread applications in game design, AR/VR, video conferencing, *etc.* This often relies on accurate 3D head reconstruction, which remains particularly challenging due to the human visual system’s sensitivity to facial details. Even subtle rendering artifacts are more noticeable on faces than on other objects. Traditional approaches rely on statistical 3D face models [Blanz and Vetter, 2023; Wang *et al.*, 2024] to generate high-fidelity 3D heads. These models can preserve facial structure and provide identity consistency across different facial expressions and perspectives, which is essential for realistic human face synthesis. However, they are typically limited to the facial region and often fail to reconstruct the full head, missing important features such as hair, glasses, and accessories.

Recent advancements in diffusion models [Ho *et al.*, 2020a; Rombach *et al.*, 2021] have led to significant progress in text-to-image generation, with several studies [Long *et al.*, 2024; Liu *et al.*, 2023; Shi *et al.*, 2023a; Wang and Shi, 2023] extending diffusion models to image-to-3D conversion. These models are trained on large-scale 3D datasets to generate multi-view images for 3D object reconstruction, making it possible to reconstruct details such as hair, glasses, and accessories more effectively. While these models are trained on large-scale 3D datasets to generate multi-view images for 3D object reconstruction, they often lack sufficient geometric and textural consistency when the input is a human face. This discrepancy becomes particularly problematic because human faces require not only geometric consistency but also the preservation of subtle features such as expression, identity, and accessories. Upon reviewing existing image-to-3D methodologies, the following primary limitations can be identified: 1) Most image-to-3D diffusion models are trained on large-scale 3D datasets [Deitke *et al.*, 2023; Deitke *et al.*, 2024], which often lack high-quality head data and suffer from a limited number of meshes, resulting in poor quality reconstructions. 2) Although existing image-to-3D diffusion models leverage view-dependent information (*e.g.*, camera parameters [Liu *et al.*, 2023], normal maps [Long *et al.*, 2024]) to guide multi-view generation, they still struggle to maintain identity and expression consistency for human head generation. This is particularly challenging because human faces require much higher consistency compared to other objects. 3) Image-to-3D diffusion models typically generate only 4-6 multi-view images, which limits the quality of subsequent 3D reconstruction. Achieving high-quality 3D model reconstruction from these limited perspectives requires complex and inefficient optimization.

To address these challenges, we enhance the existing image-to-3D methodology with several key innovations. First, we construct a digital human dataset with diverse attributes (*e.g.*, hairstyle, skin color, age, gender, accessory, expression, *etc.*) to fine-tune the multi-view diffusion model. This dataset combines real-world and virtual data, incorporating both high-quality and plausible exam-

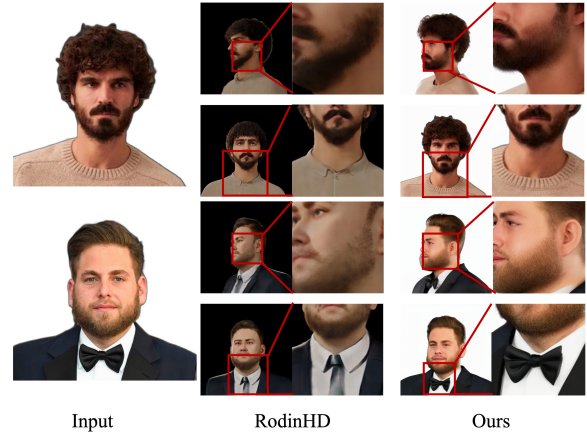


Figure 2: Compared to RodinHD [Wang *et al.*, 2023], our method demonstrates a higher degree of facial similarity and clothing consistency.

ples to mitigate the issue of insufficient high-quality human datasets. Second, we leverage the more powerful video diffusion model, [Blattmann *et al.*, 2023; Voleti *et al.*, 2025; Yang *et al.*, 2024], for multi-view generation. This model produces a larger number of consistent images with its pre-trained knowledge, which aids in the subsequent 3D reconstruction task. While diffusion models face challenges in maintaining multi-view consistency for human head generation and preserving identity, we integrate identity information into the multi-view diffusion process to improve facial consistency across views. Specifically, we apply identity-aware guidance and supervision to extract precise facial representations, which guide the model and impose objective functions to ensure high identity consistency during generation. Additionally, we enhance the facial representation network to better distinguish expressions that are disentangled from identity, providing improved expression-preserving capabilities. Finally, we employ 3D Gaussian Splatting [Kerbl *et al.*, 2023] for real-time, high-quality 3D human head rendering. Experimental results demonstrate that our proposed method generates vivid 3D human faces, especially when the input images feature extreme expressions, accessories, and non-frontal poses. In summary, the contributions of our work are as follows:

- We propose a high-quality human head dataset consisting of 227 sequences of digital human portraits captured from 96 different perspectives, totaling 21,792 frames.
- We introduce an improved 3D human head reconstruction model with identity-aware guidance and supervision, which enhances identity and expression consistency in the 3D reconstruction process.
- Our experimental results demonstrate high-fidelity 3D head generation from a single portrait image, particularly when the input images contain extreme expressions, accessories, and side profiles.

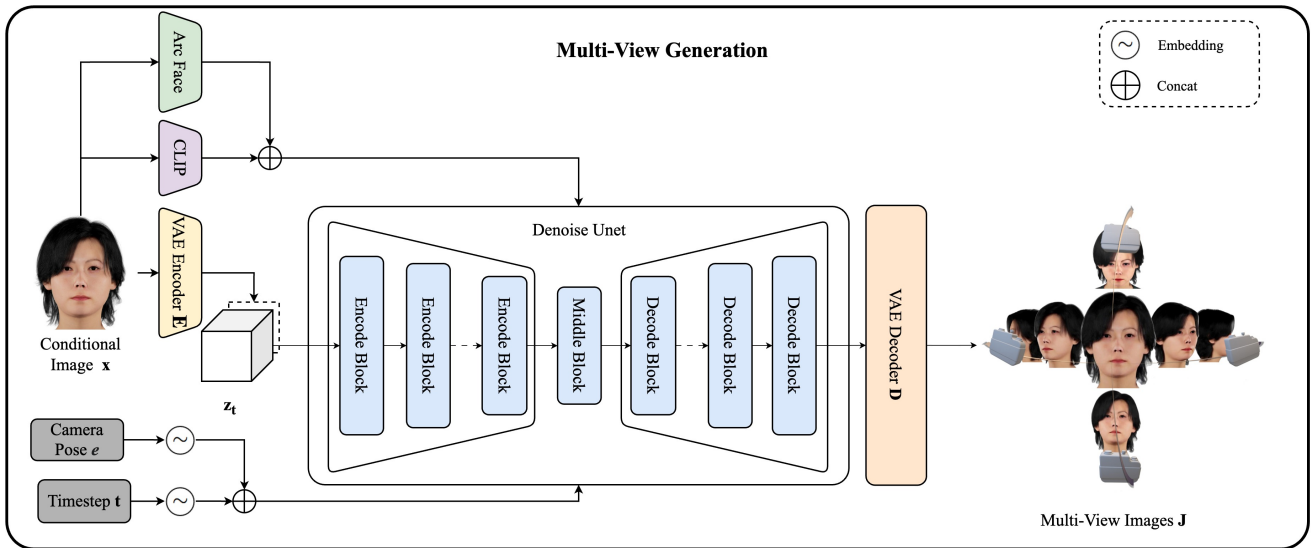


Figure 3: **Our Multi-View Generation Model.** We apply timestep embedding to camera pose e and add it to noise step t . These are then fed into the residual module of the UNet. Additionally, we input the conditional image’s CLIP embedding and ArcFace embedding into the transformer module for cross-attention. The resulting latent embedding is concatenated with the latent space state z_t .

2 Related Works

Multi-View Diffusion Models: Multi-view diffusion builds upon text-to-image diffusion, leveraging the strong 2D priors of diffusion models and achieving significant advancements through training on large-scale 3D datasets. Most methods focus their innovations on maintaining multi-view consistency. For instance, Zero123++ [Shi *et al.*, 2023a] fixes the camera viewpoint and employs a linear noise addition strategy, Wonder3D [Long *et al.*, 2024] enhances consistency by controlling the generation of multi-view normal maps and RGB images, while ImageDream [Wang and Shi, 2023] aligns text-to-3D diffusion model [Shi *et al.*, 2023b] capabilities to ensure consistency in image-to-3D synthesis. However, their performance in multi-view facial synthesis is suboptimal, and the number of generated views is highly limited, which constrains the effectiveness of downstream 3D facial reconstruction tasks. FaceLift [Lyu *et al.*, 2024] conducts training on multi-view diffusion within a large-scale avatar dataset, aiming to generate high-fidelity 3D heads. However, its input images are restricted to the frontal views of identities, which poses a constraint on the data diversity and potential application scenarios.

3D Head Generation: The 3D reconstruction of the human head from a single image has been a hot topic for an extended period, resulting in numerous high-quality contributions to the field. Many approaches [Blanz and Vetter, 2023; Chai *et al.*, 2023; Wang *et al.*, 2024] believed in two ideas: the first idea is that linear combinations of faces produce morphologically realistic faces; the second idea is the separation of facial shape and color and disentangling these from external factors such as illumination and camera. Based on the above ideas, these methods have achieved significant milestones in 3D face reconstruction. However, these methodologies synthesize only the facial features and do not include the entire head. PanoHead [An *et al.*, 2023a] builds upon

the EG3D [Chan *et al.*, 2022] method and achieves full head synthesis based on GAN [Goodfellow *et al.*, 2014]. However, since the triplane representation is implicit, the expressive capability of their model is somewhat limited. Rodin [Wang *et al.*, 2023] and RodinHD [Zhang *et al.*, 2025] incorporate a combination of the diffusion model and the triplane representation. However, their methods fail to generate fine details and exhibit lower similarity with the input image, as demonstrated in Fig. 2.

3D Reconstruction: Reconstruction algorithms have made significant progress since the advent of NeRF [Mildenhall *et al.*, 2021], which implicitly encodes a 3D scene into a neural network and renders it using volumetric functions. However, the implicit representation restricts its applications, especially in dynamic scene or object reconstruction. In the work of Neus [Wang *et al.*, 2021], the surface is modeled as the zero-level set of a signed distance function (SDF), and a new volume rendering method is developed to train a neural SDF representation. Nevertheless, this method is extremely time-consuming when training for a single scene or object. InstantNGP [Müller *et al.*, 2022] substantially reduces NeRF’s rendering time by enhancing a small neural network with a multi-resolution hash table. However, it has limited effectiveness when sparse viewpoints are input. Recently, 3D Gaussian Splatting [Kerbl *et al.*, 2023] has demonstrated promising reconstruction results with the representation of Gaussian point clouds. This approach can be utilized for modeling dynamic scenes or objects, and its rendering speed is also fast. This is why we chose it for our multi-view head 3D reconstruction.

3 Methodology

To obtain the 3D representation from a single input image, our approach comprises two stages: generating an orbital video around the head and reconstructing the 3D head model

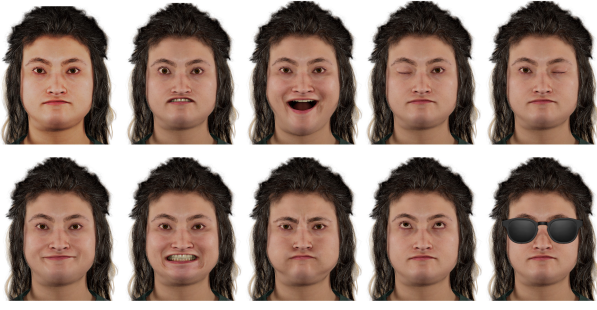


Figure 4: **Different Expressions And An Accessory.** Diverse facial expressions are sampled to enrich our dataset, along with an accessory to validate the fitting capability of our diffusion model.

using the multi-view video. First, we construct a diverse and high-quality digital 3D head dataset. This dataset features a variety of attributes, such as different hairstyles, skin tones, age groups, genders, accessories, and expressions, ensuring diversity and high realism. Then, we train a Stable Video Diffusion (SVD) model [Blattmann *et al.*, 2023] fusing our digital human dataset for multi-view image generation. The SVD model is fine-tuned to produce high-consistency, identity-aware multi-view images of the input portrait. Finally, we utilize the multi-view video generated by the SVD model to create a 3D Gaussian Splatting representation [Kerbl *et al.*, 2023]. This enables real-time, high-quality 3D head reconstruction with robust geometry and texture consistency. The overall architecture is illustrated in Fig. 3.

3.1 Problem Formulation

Given a single image $\mathbf{x} \in \mathbb{R}^{3 \times H \times W}$ of an identity \mathbf{I} and the corresponding camera elevation $\mathbf{e} \in [-10^\circ, 40^\circ]$, we encode the information into SVD. The SVD model outputs multi-view images $\mathbf{J} \in \mathbb{R}^{N_s \times 3 \times H \times W}$ around the identity \mathbf{I} , N_s denote image number. The camera positions of these output images are represented as $\pi \in \mathbb{R}^{N_s \times 2} = \{(\mathbf{e}_i, \mathbf{a}_i)\}_{i=1}^{N_s}$, where \mathbf{e}_i corresponds to the pose of each camera, equal to the input elevation \mathbf{e} , and $\mathbf{a}_i \in [0^\circ, 360^\circ]$ represents the azimuth. Finally, we utilize 3D Gaussian Splatting to reconstruct the 3D head model using the multi-view images and the corresponding camera pose trajectory.

3.2 Digital Human Head Dataset

To train our diffusion model, we sample multi-view images from the 3D models of digital human heads. Specifically, we render 1024×1024 resolution images from $N = 100$ realistic human head models. These renderings $N_e = 6$ cover elevation angles of $[-10^\circ, 0^\circ, 10^\circ, 20^\circ, 30^\circ, 40^\circ]$, azimuth angles at $N_a = 16$ positions around the head, resulting in $N_v = 96$ unique viewpoints per head. Additionally, each avatar features $N_f = 10$ appearances with 9 different expressions and 1 accessory, as is shown in Fig. 4.

3.3 Multi-View Generation

Multi-view generation is a critical step in our method, providing the essential face images from different perspectives for 3D reconstruction. The generated multi-view images must be

high-quality, identity-preserving, and appearance-consistent with the input portrait. To produce multi-view images with higher spatial-temporal consistency and more frames, we adopt the core architecture of the SVD model [Blattmann *et al.*, 2023] for multi-view head generation. SVD is pre-trained on extensive video data, inherently capturing high spatial-temporal consistency. Its UNet architecture, with spatial and temporal attention modules, effectively models the latent relationships between multi-view images. Previous works [Voleti *et al.*, 2025; Yang *et al.*, 2024] trained SVD for multi-view generation by embedding conditional images and camera positions into the denoising UNet, generating orbital videos for input objects. Building on these approaches, we incorporate identity constraints to further enhance the SVD model’s performance in head synthesis. The entire process is illustrated in Fig. ??.

Architecture: The SVD model adopts latent diffusion [Rom-bach *et al.*, 2022], where the input image is first compressed into a latent space, and then the diffusion process [Ho *et al.*, 2020b] is applied to generate high-quality images. The architecture contains VAE encoder \mathbf{E} , decoder \mathcal{D} and denoise Unet. Each UNet block includes a residual module and two transformer modules, each equipped with a temporal attention layer and a spatial attention layer. The input condition image \mathbf{x} is processed in two ways. First, it is encoded with the latent space state as $\mathbf{z}_0 = \mathbf{E}(\mathbf{x})$ produced by the VAE encoder. Then, noise is added to create the latent \mathbf{z}_t to for denoising (we omit the process of adding noise here, please refer to [Ho *et al.*, 2020b] for more details). Second, \mathbf{x} is used as guidance for the cross-attention mechanism with \mathbf{z}_t . This guidance ensures the UNet generates content aligned with the input. Typically CLIP [Radford *et al.*, 2021] embeddings are used as guidance to provide semantic information for general images. Here, we additionally employ **identity guidance**, utilizing ArcFace [Deng *et al.*, 2019] a network specifically designed for facial representation, to better preserve facial identity. At the same time, the camera pose \mathbf{e} is integrated with timestep \mathbf{t} and fed into the residual block, ultimately producing frames of multi-view surround images. The fine-tuning objective is defined as follows:

$$\min_{\theta} \mathbb{E}_{\mathbf{z} \sim \epsilon(\mathbf{x}), \mathbf{t}, \epsilon \sim N(0,1)} \|\epsilon - \epsilon_{\theta}(\mathbf{z}; \mathbf{t}, \mathbf{e}, \text{CLIP}(\mathbf{x}), \text{ArcFace}(\mathbf{x}))\|_2^2, \quad (1)$$

θ represents the network parameters, ϵ is the scheduled Gaussian noise added during training, and ϵ_{θ} is the predicted noise. The camera pose e controls the viewpoint of the multi-view images. After the latent diffusion process, the latent state is decoded by the VAE decoder D to generate the final multi-view images.

Objective Functions: To improve generalization, we randomly sample conditional images from various perspectives for each avatar and its corresponding facial expressions or accessories during training. Directly applying pixel-wise mean squared error (MSE) loss often struggles to preserve identity, expressions, and other critical characteristics. To address this, we employ a combination of MSE loss, perceptual loss and identity loss as an identity loss. The perceptual loss, inspired by [Zhang *et al.*, 2018], extracts feature stacks from the generated images \mathbf{J} with VGG network and ground truth images \mathbf{J}^* across L layers, normalizes the features along the chan-

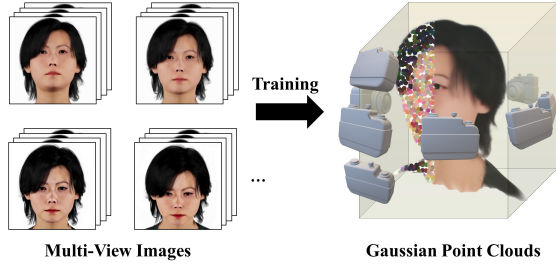


Figure 5: **3D Head Reconstruction.** Optimizing 3D Gaussian point clouds using 96 viewpoints around the head.

nel dimension, and calculates the L_2 distance of \mathbf{J} and \mathbf{J}^* as perceptual loss, which is defined as follows:

$$\mathcal{L}_{perc}(\mathbf{J}, \mathbf{J}^*) = \frac{1}{N_s} \sum_i^{N_s} \sum_l \frac{1}{H_l W_l} \sum_{h,w} \|w^l \odot (j_{ihw}^l - j_{ihw}^{*l})\|, \quad (2)$$

where $j_{ihw}^l, j_{ihw}^{*l} \in \mathbb{R}^{H_l \times W_l \times C_l}$ represent feature of \mathbf{J} and \mathbf{J}^* in l -th layer, $w^l \in \mathbb{R}^{C_l}$ represent scale factor.

The identity loss computes the cosine distance between the latent features of \mathbf{J} and \mathbf{J}^* extracted ArcFace [Deng *et al.*, 2019] network. It is defined as:

$$\mathcal{L}_{ID}(\mathbf{J}, \mathbf{J}^*) = 1 - \frac{1}{N_s} \sum_i \frac{j_i \cdot j_i^*}{\|j_i\| \|j_i^*\|}, \quad (3)$$

where j_i, j_i^* represent features of \mathbf{J} and \mathbf{J}^* .

The overall loss function is defined as:

$$\mathcal{L}_{\mathcal{M}}(\mathbf{J}, \mathbf{J}^*) = \mathcal{L}_{MSE}(\mathbf{J}, \mathbf{J}^*) + \lambda_p \mathcal{L}_{perc}(\mathbf{J}, \mathbf{J}^*) + \lambda_i \mathcal{L}_{ID}(\mathbf{J}, \mathbf{J}^*), \quad (4)$$

where \mathbf{J} and \mathbf{J}^* denote the denoised images and ground truth images, respectively, while λ_p and λ_i are loss weights.

Facial Expression Representation Enhancement: We finetune the network using pretrained weights on datasets specifically designed for facial expressions and identities to further enhance facial representation. This finetuning enables the network to classify various faces and expressions by interpreting them as identity information. ArcFace modifies the softmax function by normalizing the weights of the last layer, setting the bias to zero, and introducing a margin m to increase the gap between positive and negative samples. The updated softmax loss is defined as:

$$\mathcal{L}_{FRE}(\mathbf{J}_i) = -\log \frac{e^{s(\cos(\theta_{y_i} + m))}}{e^{s(\cos(\theta_{y_i} + m))} + \sum_{k, k \neq y_i}^{N_l} e^{s(\cos(\theta_k))}}, \quad (5)$$

where N_l represents the number of classes, y_i is the label for sample \mathbf{J}_i , s is the scaling factor, θ_k are the angles between the embedding vectors of \mathbf{J}_i and the weights of class k in the last layer. In our implementation, the label y_i is defined as a combination of identity and expression to differentiate between expressions of the same identity. Specifically, $N_l = N \times N_f$. All N_v views of images within the same identity and appearance share the same label. Through this finetuning process, the ArcFace embedding is capable of distinguishing between different expressions of the same identity while providing consistent representations across different viewing angles.

Method	LPIPS↓	PSNR↑	SSIM↑	ID↑
SV3D	0.4105	12.8437	0.5382	0.7960
Wonder3D	0.4286	10.0479	0.4883	0.7092
Hi3D	0.4171	11.3197	0.5191	0.6901
PanoHead	0.5130	8.8752	0.3665	0.5320
Ours	0.2583	17.8957	0.6661	0.8987

Table 1: Quantitative evaluation of novel multi-view synthesis.

3.4 3D Reconstruction From Multi-View Images

We reconstruct the 3D representation from the multi-view images \mathbf{J} generated by our diffusion model. For 3D head reconstruction, we adopt 3D Gaussian Splatting due to its fast training speed and memory efficiency. Specifically, we initialize with random point clouds and use $N_v = 96$ images \mathbf{J} along with their corresponding camera poses π as the training set. The rendered 2D images undergo optimization to produce the final Gaussian point cloud model. The reconstruction process is illustrated in Fig. 5. In addition to the original MES loss and SSIM loss, we have also incorporated the LPIPS loss to enhance the reconstruction effect of the detailed parts as [Chen *et al.*, 2024] did. The loss function is defined as:

$$\mathcal{L}_{\mathcal{R}}(\mathbf{J}, \mathbf{J}^*) = \mathcal{L}_{MSE}(\mathbf{J}, \mathbf{J}^*) + \lambda_s \mathcal{L}_{SSIM}(\mathbf{J}, \mathbf{J}^*) + \lambda_p \mathcal{L}_{perc}(\mathbf{J}, \mathbf{J}^*), \quad (6)$$

where λ_s, λ_p represent loss weights. Each optimization takes approximately 5 minutes on an RTX 4090 GPU, using around 2000MB of VRAM.

4 Experiments

4.1 Experimental Settings

Datasets We constructed a dataset featuring new faces and expressions for evaluation. To test the generalization ability of the methods, we selected 10 subjects with 5 expressions each and randomly chose either a side or front viewpoint as the conditional image. Our diffusion model was trained on the digital human head dataset and generated 16 images at a resolution of 512x512 pixels.

Baseline We evaluated two categories of methods. The first category includes multi-view diffusion models, such as Wonder3D [Long *et al.*, 2024], which is based on stable diffusion, and SV3D [Voleti *et al.*, 2025] and Hi3D [Yang *et al.*, 2024], which are grounded in stable video diffusion. The second category includes 3D human head generation methods, represented by PanoHead [An *et al.*, 2023b], the state-of-the-art method based on 3D GANs.

Evaluation Metric We compared each generated frame with its corresponding ground truth frame using LPIPS [Zhang *et al.*, 2018], PSNR, SSIM, ArcFace [Deng *et al.*, 2019]. These metrics collectively assess both pixel-level accuracy and identity preservation.

4.2 Comparison with Other Methods

We evaluated the fidelity of our multi-view images against the outputs of SV3D [Voleti *et al.*, 2025], Wonder3D [Long *et al.*, 2024], Hi3D [Yang *et al.*, 2024] and PanoHead [An

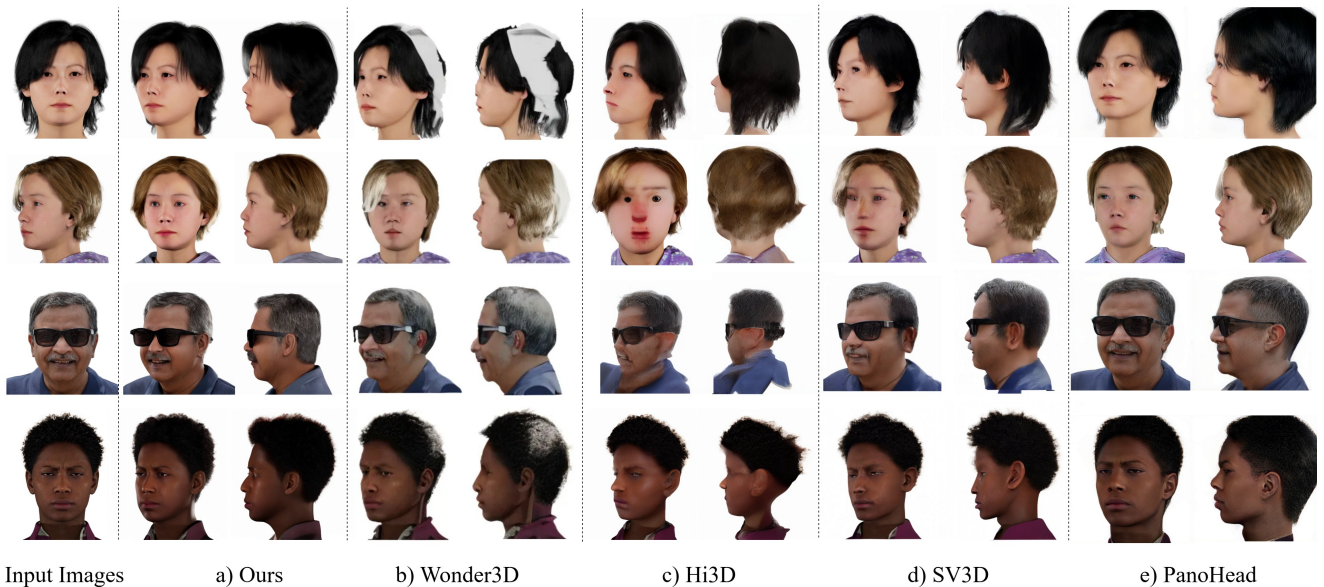


Figure 6: **Visual Comparison With Other Methods.** Compared to other models, our method effectively preserves multi-view consistency across all viewpoints and expressions, including scenarios with accessories.

Method	LPIPS↓	PSNR↑	SSIM↑	ID↑
Finetuned	0.2639	17.7205	0.6633	0.8929
+L	0.2629	17.5756	0.6668	0.8927
+G	0.2605	17.8393	0.6662	0.8973
+L+G	0.2632	17.6710	0.6646	0.8947
+L+G+E	0.2583	17.8957	0.6661	0.8987

Table 2: **Ablation Results.** “L” represents identity loss, “G” represents identity guidance, “E” represents with facial expression representation enhancement.

et al., 2023b], as is shown in Tab.1. Our approach consistently achieved higher scores across all evaluation metrics. Compared to other models, our method exhibits a remarkable ability to maintain multi-view consistency and high fidelity across any viewpoint and facial expression, including scenarios with accessories. Specifically, Wonder3D struggled with reconstructing hair and sunglasses. Hi3D failed to generate complete facial regions. SV3D exhibited low identity preservation and weak similarity to the input. PanoHead produced sub-optimal results, especially for side-view faces.

A visual comparison is presented in Fig.6. From the results, it is evident that most of the other models fail to generate images with clear human characteristics. Issues such as distorted face shapes and poor identity preservation are especially pronounced when the input image is non-frontal.

4.3 Ablative Analyses

To validate the effectiveness of identity and expression information constraints, we conducted ablation experiments with different configurations. The base model was fine-tuned on our proposed dataset, and we tested three types of identity/expression modules: identity loss (“L”), identity guid-

ance (“G”), and Facial Expression Representation Enhancement (“E”). We evaluated five different methods for integrating identity information and compared their performance on the test set at the same training step. The results, summarized in Tab. 2, demonstrate that the combination of fine-tuning on our proposed dataset, identity loss, and identity embedding guidance using facial expression representation enhancement achieves optimal performance across most metrics.

4.4 Generalization Results

We evaluated our model’s performance on facial expressions it had not encountered during training. A selection of generated results is shown in Fig. 7. *Due to space constraints, additional results, including videos of 3D reconstruction, are provided in the supplementary materials.* These results demonstrate that our method maintains facial consistency across multiple viewpoints while effectively preserving detailed facial expressions. To assess the model’s ability to reconstruct 3D human heads from arbitrary viewpoints, we tested its performance on extreme side-view images of human faces. The experiments reveal that our method can infer frontal face information from limited facial data and synthesize 3D portraits, achieving high facial consistency and restoring a substantial amount of facial detail. Additionally, we tested our method on the real-world facial dataset FFHQ [Karras, 2019], which includes faces with complex lighting, environmental conditions, and diverse facial features. The generated results indicate that our method demonstrates strong generalization performance on this dataset.

In the supplementary materials, we also showcase how our method supports the synthesis of 4D human heads.

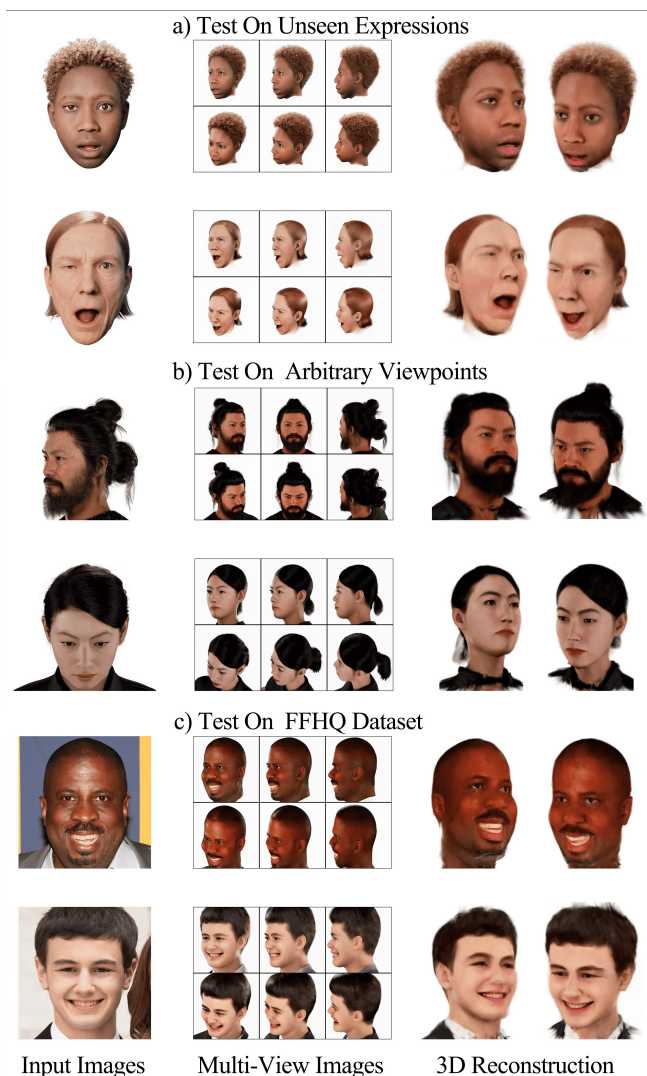


Figure 7: Testing our method on unseen expressions, arbitrary viewpoints, and the FFHQ dataset.

5 Conclusions

We present a novel high-fidelity 3D head reconstruction method from a single portrait image, independent of its perspective, expression, or the presence of accessories. We introduce a new multi-view digital human dataset that includes a large number of subjects with diverse expressions. Our approach involves generating multi-view images around the input identity and reconstructing a 3D representation using 3D Gaussian Splatting. Compared with existing methods, our approach achieves superior results in head reconstruction.

References

- [An *et al.*, 2023a] Sizhe An, Hongyi Xu, Yichun Shi, Guoxian Song, Umit Y Ogras, and Linjie Luo. Panohead: Geometry-aware 3d full-head synthesis in 360deg. In *Proceedings of the IEEE/CVF conference on computer vision and pattern recognition*, pages 20950–20959, 2023.
- [An *et al.*, 2023b] Sizhe An, Hongyi Xu, Yichun Shi, Guoxian Song, Umit Y Ogras, and Linjie Luo. Panohead: Geometry-aware 3d full-head synthesis in 360deg. In *Proceedings of the IEEE/CVF conference on computer vision and pattern recognition*, pages 20950–20959, 2023.
- [Blanz and Vetter, 2023] Volker Blanz and Thomas Vetter. A morphable model for the synthesis of 3d faces. In *Seminal Graphics Papers: Pushing the Boundaries, Volume 2*, pages 157–164. 2023.
- [Blattmann *et al.*, 2023] Andreas Blattmann, Tim Dockhorn, Sumith Kulal, Daniel Mendeleevitch, Maciej Kilian, Dominik Lorenz, Yam Levi, Zion English, Vikram Voleti, Adam Letts, et al. Stable video diffusion: Scaling latent video diffusion models to large datasets. *arXiv preprint arXiv:2311.15127*, 2023.
- [Chai *et al.*, 2023] Zenghao Chai, Tianke Zhang, Tianyu He, Xu Tan, Tadas Baltrusaitis, HsiangTao Wu, Runnan Li, Sheng Zhao, Chun Yuan, and Jiang Bian. Hiface: High-fidelity 3d face reconstruction by learning static and dynamic details. In *Proceedings of the IEEE/CVF International Conference on Computer Vision*, pages 9087–9098, 2023.
- [Chan *et al.*, 2022] Eric R Chan, Connor Z Lin, Matthew A Chan, Koki Nagano, Boxiao Pan, Shalini De Mello, Orazio Gallo, Leonidas J Guibas, Jonathan Tremblay, Sameh Khamis, et al. Efficient geometry-aware 3d generative adversarial networks. In *Proceedings of the IEEE/CVF conference on computer vision and pattern recognition*, pages 16123–16133, 2022.
- [Chen *et al.*, 2024] Zilong Chen, Yikai Wang, Feng Wang, Zhengyi Wang, and Huaping Liu. V3d: Video diffusion models are effective 3d generators. *arXiv preprint arXiv:2403.06738*, 2024.
- [Deitke *et al.*, 2023] Matt Deitke, Dustin Schwenk, Jordi Salvador, Luca Weihs, Oscar Michel, Eli VanderBilt, Ludwig Schmidt, Kiana Ehsani, Aniruddha Kembhavi, and Ali Farhadi. Objaverse: A universe of annotated 3d objects. In *Proceedings of the IEEE/CVF Conference on Computer Vision and Pattern Recognition*, pages 13142–13153, 2023.
- [Deitke *et al.*, 2024] Matt Deitke, Ruoshi Liu, Matthew Wallingford, Huong Ngo, Oscar Michel, Aditya Kusupati, Alan Fan, Christian Laforte, Vikram Voleti, Samir Yitzhak Gadre, et al. Objaverse-xl: A universe of 10m+ 3d objects. *Advances in Neural Information Processing Systems*, 36, 2024.
- [Deng *et al.*, 2019] Jiankang Deng, Jia Guo, Niannan Xue, and Stefanos Zafeiriou. Arcface: Additive angular margin loss for deep face recognition. In *Proceedings of the IEEE/CVF conference on computer vision and pattern recognition*, pages 4690–4699, 2019.
- [Goodfellow *et al.*, 2014] Ian Goodfellow, Jean Pouget-Abadie, Mehdi Mirza, Bing Xu, David Warde-Farley, Sherjil Ozair, Aaron Courville, and Yoshua Bengio. Generative adversarial nets. *Advances in neural information processing systems*, 27, 2014.

- [Ho *et al.*, 2020a] Jonathan Ho, Ajay Jain, and Pieter Abbeel. Denoising diffusion probabilistic models. *Advances in neural information processing systems*, 33:6840–6851, 2020.
- [Ho *et al.*, 2020b] Jonathan Ho, Ajay Jain, and Pieter Abbeel. Denoising diffusion probabilistic models. *Advances in neural information processing systems*, 33:6840–6851, 2020.
- [Karras, 2019] Tero Karras. A style-based generator architecture for generative adversarial networks. *arXiv preprint arXiv:1812.04948*, 2019.
- [Kerbl *et al.*, 2023] Bernhard Kerbl, Georgios Kopanas, Thomas Leimkühler, and George Drettakis. 3d gaussian splatting for real-time radiance field rendering. *ACM Trans. Graph.*, 42(4):139–1, 2023.
- [Liu *et al.*, 2023] Ruoshi Liu, Rundi Wu, Basile Van Hoorick, Pavel Tokmakov, Sergey Zakharov, and Carl Vondrick. Zero-1-to-3: Zero-shot one image to 3d object. In *Proceedings of the IEEE/CVF international conference on computer vision*, pages 9298–9309, 2023.
- [Long *et al.*, 2024] Xiaoxiao Long, Yuan-Chen Guo, Cheng Lin, Yuan Liu, Zhiyang Dou, Lingjie Liu, Yuexin Ma, Song-Hai Zhang, Marc Habermann, Christian Theobalt, et al. Wonder3d: Single image to 3d using cross-domain diffusion. In *Proceedings of the IEEE/CVF Conference on Computer Vision and Pattern Recognition*, pages 9970–9980, 2024.
- [Lyu *et al.*, 2024] Weijie Lyu, Yi Zhou, Ming-Hsuan Yang, and Zhixin Shu. Facelift: Single image to 3d head with view generation and gs-lrm, 2024.
- [Mildenhall *et al.*, 2021] Ben Mildenhall, Pratul P Srinivasan, Matthew Tancik, Jonathan T Barron, Ravi Ramamoorthi, and Ren Ng. Nerf: Representing scenes as neural radiance fields for view synthesis. *Communications of the ACM*, 65(1):99–106, 2021.
- [Müller *et al.*, 2022] Thomas Müller, Alex Evans, Christoph Schied, and Alexander Keller. Instant neural graphics primitives with a multiresolution hash encoding. *ACM Trans. Graph.*, 41(4):102:1–102:15, July 2022.
- [Radford *et al.*, 2021] Alec Radford, Jong Wook Kim, Chris Hallacy, Aditya Ramesh, Gabriel Goh, Sandhini Agarwal, Girish Sastry, Amanda Askell, Pamela Mishkin, Jack Clark, et al. Learning transferable visual models from natural language supervision. In *International conference on machine learning*, pages 8748–8763. PMLR, 2021.
- [Rombach *et al.*, 2021] Robin Rombach, Andreas Blattmann, Dominik Lorenz, Patrick Esser, and Björn Ommer. High-resolution image synthesis with latent diffusion models, 2021.
- [Rombach *et al.*, 2022] Robin Rombach, Andreas Blattmann, Dominik Lorenz, Patrick Esser, and Björn Ommer. High-resolution image synthesis with latent diffusion models. In *Proceedings of the IEEE/CVF conference on computer vision and pattern recognition*, pages 10684–10695, 2022.
- [Shi *et al.*, 2023a] Ruoxi Shi, Hansheng Chen, Zhuoyang Zhang, Minghua Liu, Chao Xu, Xinyue Wei, Linghao Chen, Chong Zeng, and Hao Su. Zero123++: a single image to consistent multi-view diffusion base model. *arXiv preprint arXiv:2310.15110*, 2023.
- [Shi *et al.*, 2023b] Yichun Shi, Peng Wang, Jianglong Ye, Mai Long, Kejie Li, and Xiao Yang. Mvdream: Multi-view diffusion for 3d generation. *arXiv preprint arXiv:2308.16512*, 2023.
- [Voleti *et al.*, 2025] Vikram Voleti, Chun-Han Yao, Mark Boss, Adam Letts, David Pankratz, Dmitry Tochilkin, Christian Laforte, Robin Rombach, and Varun Jampani. Sv3d: Novel multi-view synthesis and 3d generation from a single image using latent video diffusion. In *European Conference on Computer Vision*, pages 439–457. Springer, 2025.
- [Wang and Shi, 2023] Peng Wang and Yichun Shi. Image-dream: Image-prompt multi-view diffusion for 3d generation. *arXiv preprint arXiv:2312.02201*, 2023.
- [Wang *et al.*, 2021] Peng Wang, Lingjie Liu, Yuan Liu, Christian Theobalt, Taku Komura, and Wenping Wang. Neus: Learning neural implicit surfaces by volume rendering for multi-view reconstruction. *arXiv preprint arXiv:2106.10689*, 2021.
- [Wang *et al.*, 2023] Tengfei Wang, Bo Zhang, Ting Zhang, Shuyang Gu, Jianmin Bao, Tadas Baltrusaitis, Jingjing Shen, Dong Chen, Fang Wen, Qifeng Chen, et al. Rodin: A generative model for sculpting 3d digital avatars using diffusion. In *Proceedings of the IEEE/CVF conference on computer vision and pattern recognition*, pages 4563–4573, 2023.
- [Wang *et al.*, 2024] Zidu Wang, Xiangyu Zhu, Tianshuo Zhang, Baiqin Wang, and Zhen Lei. 3d face reconstruction with the geometric guidance of facial part segmentation. In *Proceedings of the IEEE/CVF Conference on Computer Vision and Pattern Recognition*, pages 1672–1682, 2024.
- [Yang *et al.*, 2024] Haibo Yang, Yang Chen, Yingwei Pan, Ting Yao, Zhineng Chen, Chong-Wah Ngo, and Tao Mei. Hi3d: Pursuing high-resolution image-to-3d generation with video diffusion models. In *Proceedings of the 32nd ACM International Conference on Multimedia*, pages 6870–6879, 2024.
- [Zhang *et al.*, 2018] Richard Zhang, Phillip Isola, Alexei A Efros, Eli Shechtman, and Oliver Wang. The unreasonable effectiveness of deep features as a perceptual metric. In *Proceedings of the IEEE conference on computer vision and pattern recognition*, pages 586–595, 2018.
- [Zhang *et al.*, 2025] Bowen Zhang, Yiji Cheng, Chunyu Wang, Ting Zhang, Jiaolong Yang, Yansong Tang, Feng Zhao, Dong Chen, and Baining Guo. Rodinhd: High-fidelity 3d avatar generation with diffusion models. In *European Conference on Computer Vision*, pages 465–483. Springer, 2025.